

Dynamics of correlated transfer-ionization in collisions with a fast highly charged ion

A.B.Voitkiv

Max-Planck-Institut für Kernphysik, Saupfercheckweg 1, D-69117 Heidelberg, Germany

Abstract

Transfer-ionization in fast collisions between a bare ion and an atom, in which one of the atomic electrons is captured by the ion whereas another one is emitted, crucially depends on dynamic electron-electron correlations. We show that in collisions with a highly charged ion a strong field of the ion has a very profound effect on the correlated channels of transfer-ionization. In particular, this field weakens electron emission into the direction opposite to the motion of the ion and strongly suppresses the emission perpendicular to this motion. Instead, electron emission is redirected into those parts of the momentum space which are very weakly populated in fast collisions with low charged ions.

PACS numbers: PACS:34.10.+x, 34.50.Fa

I. INTRODUCTION

Electron-electron interaction is responsible for very many phenomena studied by the different fields of physics ranging from astrophysics to biophysics. Amongst them atomic physics and its part – physics of ion-atom collisions – often deal with most basic and clear manifestations of this interaction.

Atomic excitation and ionization [1]-[4], projectile-electron excitation and loss [2]-[3], [5], electron transfer (capture) [1], [4] and pair production [1], [4]-[5] belong to the elementary reactions occurring when a projectile-ion collides with a target-atom. A combination of these reactions in a single-collision event is also possible and in such a case the electron-electron interaction during the collision when the external field is rapidly changing (dynamic electron correlations) is often crucial.

In particular, mutual ionization in which both a target-atom and a (partially stripped) projectile-ion eject electrons, and transfer-ionization in which one of the atomic electrons is captured by a projectile-ion whereas another one is emitted, represent processes where dynamic electron correlations play a crucial role [2]-[3], [5], [6], [7]-[8].

Transfer-ionization in fast collisions of low charged ions (mainly protons) with helium is attracting much attention [9]-[18]. This process can be analyzed in terms of different reaction mechanisms which are characterized by distinct features in the electron emission pattern. Depending on whether the electron-electron interaction plays in them a crucial role, these mechanisms can be termed "correlated" or "uncorrelated".

Uncorrelated mechanisms are independent transfer-ionization (ITI) and capture-shake-off (C-SO). In the ITI electron capture and emission occur due to "independent" interactions of the projectile with two target electrons. According to the C-SO, a fast transfer of one electron from the atom to the ion leads to a "sudden" change of the atomic potential for another electron that leads to its emission. Both ITI and C-SO result in emission of low-energy electrons.

The correlated mechanisms include electron-electron Thomas (EET) and electron-electron Auger (EEA).

Within the EET transfer-ionization proceeds [7], [19]-[20] via a binary collision of the projectile with one of atomic electrons and a consequent rescattering of this electron on another atomic electron. After these two collisions one of the electrons moves together with the projectile (that makes capture probable) while the other is emitted perpendicular to the projectile motion.

The functioning of the EEA mechanism is based on the fact that merely the presence of the projectile makes the target unstable with respect to a kind of Auger decay. Indeed, viewing the collision in the rest frame of the projectile we can see that one of the electrons, belonging initially to a bound configuration of moving particles constituting the atom, can make a transition into a bound state of the ion by transferring the energy excess to another atomic electron which, as a result of this, is emitted from the atom in the direction of the atomic motion [8], [14]. In the rest frame of the atom this electron finally moves in the direction opposite to the projectile velocity [8], [14], [16].

The mechanisms, briefly discussed above, were proposed for describing transfer-ionization in collisions between a light atom and a low charged ion moving with a velocity v , which is much higher than the typical orbiting velocities of the electron(s) in their initial and final bound states: $v \gg Z_a|e|\hbar$ and $v \gg Z_i|e|\hbar$, where Z_a and Z_i are the charges of the nuclei of the atom and ion, respectively.

What, however, can one say about transfer-ionization in fast collisions with highly charged ions (HCIs) when the charge Z_i of the ion is so large that $Z_i \sim \hbar v/|e|$? One can expect that in such collisions, which are characterized by very strong fields generated by the HCI, not only cross sections for transfer-ionization would be much larger than in collisions with equivelocity low charged ions but also new interesting features could arise in this process.

Therefore, in this article we explore transfer-ionization in fast collisions with HCIs. It will be seen below that a strong field of HCI has a dramatic effect on the correlated channels of transfer ionization: it weakens the EEA, eliminates the EET and leads to qualitatively new structures in the emission spectrum. Atomic units ($\hbar = m_e = |e| = 1$) are used throughout except where

the otherwise stated.

II. GENERAL CONSIDERATION

A. Correlated transfer-ionization

We are mainly interested in the correlated transfer-ionization and begin with its treatment. This treatment will be semiclassical in which only the electrons are described quantum mechanically whereas the heavy particles (the nuclei of the ion and atom) are considered classically. In fast collisions the trajectories of the heavy particles are practically straight-line. It is convenient to make the basic consideration of the correlated transfer-ionization using the rest frame of the ion and to take its position as the origin.

According to scattering theory the exact (semiclassical) transition amplitude can be written as

$$a_{fi} = -i \int_{-\infty}^{+\infty} dt \langle \psi_f(t) | \hat{W}(t) | \Psi_i^{(+)}(t) \rangle. \quad (1)$$

Here $\Psi_i^{(+)}$ is an exact solution of the time-dependent Schrödinger equation with the full Hamiltonian \hat{H} which describes two electrons moving in the external field of the nuclei and interacting with each other, ψ_f denotes the final state of the two electrons and \hat{W} is that part of \hat{H} which is not included into the wave equation for ψ_f . Since the contribution to transfer-ionization from collisions, in which electrons change spin, is negligible we shall disregard the spin parts of the states Ψ_i and ψ_f .

In the correlated transfer-ionization the velocities of the electrons with respect to the nucleus of the atom in the final state are of the order of v [16]. Besides, in this state the relative velocity of the electrons is also of the same order. Therefore, when this process occurs in fast collisions with HCIs, for which one has $Z_i \sim v$ but $\max\{Z_a, 1\} \ll v$, the motion of both electrons in the final state ψ_f is driven by the field of the HCI whereas the interactions of the electrons with the atomic nucleus and with each other can be neglected. Thus, we have

$$\begin{aligned} \psi_f(t) &= \frac{1}{\sqrt{2}} (\chi_b(\mathbf{r}_1) \chi_{\mathbf{p}}(\mathbf{r}_2) \pm \chi_b(\mathbf{r}_2) \chi_{\mathbf{p}}(\mathbf{r}_1)) \\ &\times \exp(-i(\varepsilon_f + p^2/2)t), \end{aligned} \quad (2)$$

where \mathbf{r}_1 and \mathbf{r}_2 are the coordinates of the electrons, χ_b is the bound state of an electron captured by the HCI with an energy ε_f and $\chi_{\mathbf{p}}$ is the state of emitted electron which moves in the HCI's field and has asymptotically a momentum \mathbf{p} .

When the state ψ_f is taken in the form (2) the perturbation \hat{W} in Eq.(1) is equal to $\hat{W}_{1a} + \hat{W}_{2a} + \hat{W}_{12}$, where \hat{W}_{ja} ($j = 1, 2$) is the interaction between the j -th electron and the nucleus of the atom and \hat{W}_{12} is the

electron-electron interaction. Then we obtain

$$\begin{aligned} a_{fi} &= -i \int_{-\infty}^{+\infty} dt \langle \psi_f(t) | \hat{W}_{1a} + \hat{W}_{2a} | \Psi_i^{(+)}(t) \rangle \\ &\quad -i \int_{-\infty}^{+\infty} dt \langle \psi_f(t) | \hat{W}_{12} | \Psi_i^{(+)}(t) \rangle, \end{aligned} \quad (3)$$

It is the last term on the right-hand side of Eq.(3) which is relevant for the correlated transfer-ionization.

In order to find a suitable approximation for $\Psi_i^{(+)}(t)$ let us note the following. In the process of correlated transfer-ionization occurring in very fast collisions ($v \gg Z_a$) both electrons undergo transitions in which the change in their momenta is much larger than their typical momenta in the initial atomic state. Because of that, even if the projectile would have a low charge, the nucleus of the atom would be merely a spectator during this process [16]. Under such circumstances the so called impulse approximation, in which the role of the atomic nucleus is just to produce the momentum distribution (and binding energy) of the electrons in the initial state, can be used to treat transfer-ionization.

In our case, in which transfer-ionization occurs in very asymmetric collisions where the charge of the HCI is much higher than the charge of the atomic nucleus, the impulse approximation is even more appropriate because it enables one to fully account for the influence of the strong field of the HCI on *two electrons*.

The initial (undistorted) atomic two-electron state is given by

$$\begin{aligned} \Psi_i^0(t) &= \varphi_a(\mathbf{r}_1 - \mathbf{R}_a(t), \mathbf{r}_2 - \mathbf{R}_a(t)) \exp(i\mathbf{v}_a \cdot (\mathbf{r}_1 + \mathbf{r}_2)) \\ &\quad \times \exp(-iv_a^2 t) \exp(-i\epsilon_a t), \end{aligned} \quad (4)$$

where $\mathbf{R}_a(t) = \mathbf{b} + \mathbf{v}_a t$ is a straight-line classical trajectory of the atomic nucleus moving with a velocity \mathbf{v}_a and φ_a is the initial atomic state with an energy ϵ_a (as viewed in the rest frame of the atom).

Now we perform the three-dimensional Fourier transformation of the state $\varphi_a(\mathbf{r}_1 - \mathbf{R}_a(t), \mathbf{r}_2 - \mathbf{R}_a(t))$, insert the obtained result into Eq.(4) and replace the plane-wave factors in the integrand by the corresponding Coulomb waves in the field of the HCI. In such a way we approximate the state $\Psi_i^{(+)}(t)$ in Eq.(3) by

$$\begin{aligned} \Psi_i^{IA}(t) &= \frac{\exp(-i(v_a^2 + \epsilon_a)t)}{(2\pi)^3} \int d^3\boldsymbol{\kappa}_1 \int d^3\boldsymbol{\kappa}_2 \phi_a(\boldsymbol{\kappa}_1, \boldsymbol{\kappa}_2) \\ &\quad \times \exp(-i(\boldsymbol{\kappa}_1 + \boldsymbol{\kappa}_2) \cdot \mathbf{R}_a(t)) \chi_{\mathbf{p}_1}(\mathbf{r}_1) \chi_{\mathbf{p}_2}(\mathbf{r}_2) \end{aligned} \quad (5)$$

Here ϕ_a is the Fourier transform of the state φ_a , $\mathbf{p}_1 = \mathbf{v}_a + \boldsymbol{\kappa}_1$ and $\mathbf{p}_2 = \mathbf{v}_a + \boldsymbol{\kappa}_2$ are the initial momenta of the electrons with respect to the HCI and $\chi_{\mathbf{p}_j}(\mathbf{r}_j)$ ($j = 1, 2$) are Coulomb wave functions of electrons which move in the field of the HCI being incident on it with asymptotic momenta \mathbf{p}_j .

Using Eqs.(2)-(3) and (5) and assuming that the space part of the initial atomic state is symmetric with respect to the interchange of the electrons (like it is the case for

the ground state of helium) one can show, after some algebra, that in the projectile frame the cross section for transfer-ionization differential in the momentum \mathbf{p} of the emitted electron is given by

$$\frac{d\sigma}{d^3\mathbf{p}} = \frac{1}{16\pi^2 v^2} \int d^2\mathbf{q}_\perp \left| \int d^3\kappa \phi_a \left(\frac{\mathbf{q} + \kappa}{2}, \frac{\mathbf{q} - \kappa}{2} \right) W_{fi} \right|^2. \quad (6)$$

In this expression

$$\mathbf{q} = \left(\mathbf{q}_\perp, \frac{\varepsilon_f + p^2/2 - v_a^2 - \varepsilon_i}{v_a} \right) \quad (7)$$

is the momentum transfer in the collision with \mathbf{q}_\perp being its transverse part ($\mathbf{q}_\perp \cdot \mathbf{v}_a = 0$) and

$$W_{fi} = \langle \chi_b(\mathbf{r}_1) \chi_{\mathbf{p}}(\mathbf{r}_2) \left| \frac{1}{r_{12}} \right| \chi_{\mathbf{p}_1}(\mathbf{r}_1) \chi_{\mathbf{p}_2}(\mathbf{r}_2) \rangle, \quad (8)$$

where $\mathbf{p}_1 = \mathbf{v}_a + (\mathbf{q} + \kappa)/2$ and $\mathbf{p}_2 = \mathbf{v}_a + (\mathbf{q} - \kappa)/2$.

Expression (6) can be drastically simplified by using the fact that the Fourier transform $\phi_a((\mathbf{q} + \kappa)/2, (\mathbf{q} - \kappa)/2)$ becomes very small when the absolute values of $\mathbf{q} \pm \kappa$ substantially exceed the typical electron velocities inside the atom. Since we consider collision velocities, which are much higher than the latter ones, we may set in Eq.(8) $\mathbf{p}_1 = \mathbf{p}_2 = \mathbf{v}_a$ and take $|W_{fi}|^2$ in Eq.(6) out of the integrals.

B. Uncorrelated transfer-ionization

Let us now say few words about the treatment of the uncorrelated channels of transfer-ionization. Following [8], [14] and [16] we shall present the amplitude for this process as the product of single-electron transition amplitudes for capture and ionization which are obtained using three-body models: continuum-distorted-wave (for capture) and continuum-distorted-wave-eikonal-initial-state (for ionization) [4].

Because of a high charge of the projectile the C-SO, compared to the ITI, contributes negligibly. Since the emission produced by these channels is localized in the same part of the momentum space the C-SO can safely be neglected.

III. RESULTS AND DISCUSSION

In figures 1-2 we present results [21] for the momentum spectrum of electrons emitted in transfer-ionization in collisions of 22.5 MeV/u Ca^{20+} projectiles ($v = 30$ a.u.) with helium atoms when capture occurs into the K and L shells. The spectrum is given in the rest frame of the target (= the laboratory frame) in which the projectile

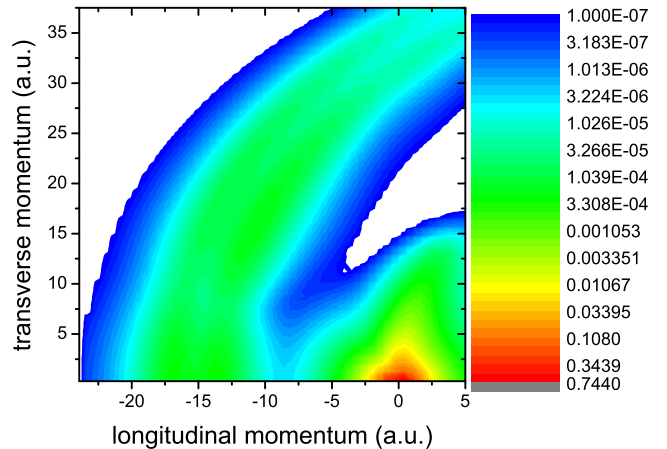


FIG. 1: Momentum spectrum (in $\text{b}/(\text{a.u.})^3$) of electrons emitted in the reactions $22.5 \text{ MeV } \text{Ca}^{20+} + \text{He}(1s^2) \rightarrow \sum_{n=1}^2 \text{Ca}^{19+}(n) + \text{He}^{2+} + e^{-}$ collisions ($v = 30$ a.u.).

moves with a velocity \mathbf{v} and is represented by the doubly differential cross section

$$\frac{d^2\sigma}{k_{tr} dk_{lg} dk_{tr}} = \int_0^{2\pi} d\varphi_k \int d^2\mathbf{q}_\perp |S_{fi}(\mathbf{q}_\perp)|^2, \quad (9)$$

where $k_{lg} = \mathbf{k} \cdot \mathbf{v}/v$ and $\mathbf{k}_{tr} = \mathbf{k} - k_{lg} \mathbf{v}/v$ are the longitudinal and transverse parts, respectively, of the momentum \mathbf{k} of the emitted electron in the laboratory frame and $k_{tr} = |\mathbf{k}_{tr}|$. The integration in (9) runs over the transverse part of the momentum transfer and the azimuthal angle φ_k of the emitted electron.

In figure 1 the maximum at small momenta has its origin in the ITI whereas the maxima at much larger k appear due to the correlated channels. The maximum at small momenta yields a very important contribution to the total cross section. However, its structure is similar to that in fast collisions with low charged projectiles, studied in [16], and below will not be considered.

The maxima at large k deserve more attention. In order to see better their structure, in figure 2 only the high-momentum part of the emission, which is produced solely via the correlated channels, is shown.

In the rest frame of the ion the approximate energy balance for transfer-ionization is very simple: $v^2 + \varepsilon_a \approx \varepsilon_f + p^2/2$, where $\varepsilon_f = -Z_i^2/2n^2$ with n being the principal quantum number of the bound state of the captured electron. Since $\mathbf{k}_{tr} = \mathbf{p}_{tr}$ and $k_{lg} = v - p_{lg}$, where \mathbf{p}_{tr} and p_{lg} are respectively the transverse and longitudinal parts of \mathbf{p} , in the target frame the emission is concentrated on ridges located along rings with radii $R_n = \sqrt{2v^2 + \varepsilon_a + Z_i^2/2n^2}$ centered at $(k_{lg} = v, k_{tr} = 0)$. The ridge with higher energy appears due to transfer-ionization with electron capture into the ground state of the projectile while the other ridge originates from capture into the projectile's L -shell. It is seen in the figure that each of these ridges has two distinct maxima: one centered at an emission angle of $\vartheta_k = 180^\circ$ and

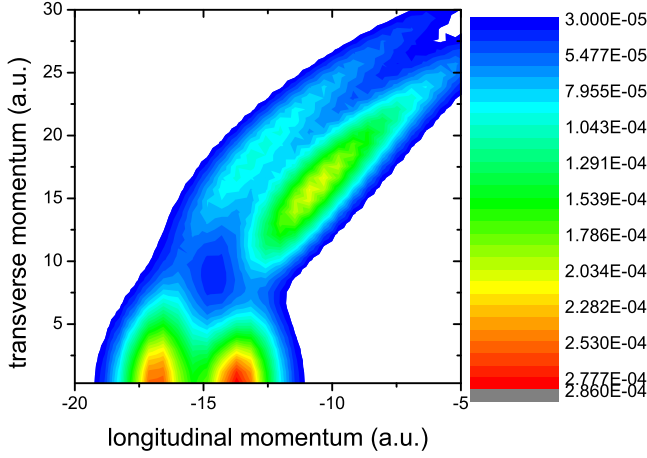


FIG. 2: Same collision system as in figure 1 but only the emission via the correlated channels is shown.

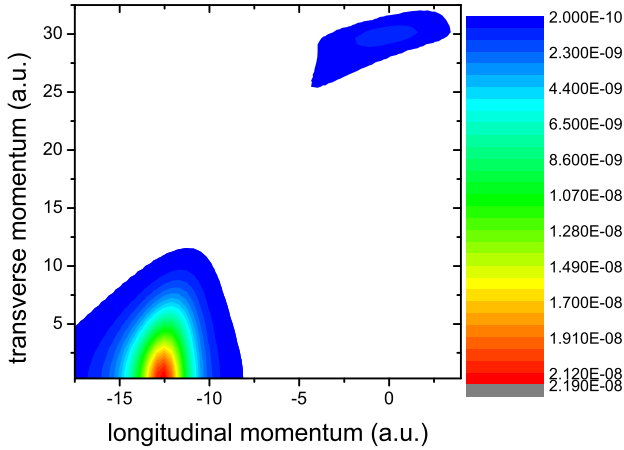


FIG. 3: Momentum spectrum (in $b/(a.u.)^3$) of electrons emitted via the correlated mechanisms in the reaction $22.5 \text{ MeV } p^+ + \text{He}(1s^2) \rightarrow \text{H}(1s) + \text{He}^{2+} + e^-$.

the other at $\vartheta_k \approx 125^\circ$ (the angle ϑ_k is counted from the direction of the projectile motion).

The shape of the correlated part of the spectrum in case of collisions with HCIs is to be compared with that in collisions with low charged ions. The latter is displayed in figure 3 for $22.5 \text{ MeV } p^+ + \text{He}(1s^2)$ collisions. Since at $Z_i \ll v$ transfer-ionization is strongly dominated by capture into the ground state this spectrum [22] is concentrated on a single ridge. Compared to the corresponding ridge in 2 the ridge in figure 3 is shifted to lower k because of the much smaller binding energy of the captured electron. It consists of two distinct parts: the maximum at $\vartheta_k = 180^\circ$ is caused by the EEA whereas the maximum at $\vartheta_k \approx 90^\circ$ is the signature of the EET.

Comparing the spectra in figures 2 and 3, one can attribute the maxima at $\vartheta_k = 180^\circ$ in figure 2 as arising due to the EEA. However, in the strong-field regime there is no maximum at $\vartheta_k \approx 90^\circ$ which is characteristic of the EET channel in collisions with fast low-charged ions. Instead, a new maximum appears on each ridge at

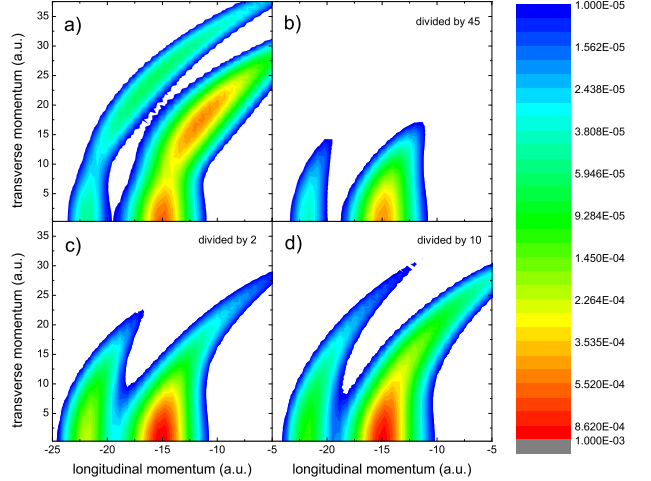


FIG. 4: The momentum spectra for the reactions $22.5 \text{ MeV/u } \text{Zn}^{30+} + \text{He}(1s^2) \rightarrow \sum_{n=1}^2 \text{Zn}^{29+}(n) + \text{He}^{2+} + e^-$.

$\vartheta_k \approx 125^\circ$ which is absent when the projectile has a low charge. This maximum is rather intense and its contribution to the total cross section is comparable to (or even exceeds) that of the EEA maximum.

In order to get more ideas about the correlated transfer-ionization in the strong-field regime, in figure 4 we present the emission spectrum at even a stronger field when $22.5 \text{ MeV/u } \text{Zn}^{30+}$ projectiles collide with helium. As before, we consider capture into the K and L shells only. From figure 4a it can be inferred that the structure of the spectrum is similar to that in collisions with Ca^{20+} ions: it has two ridges and each of them has two pronounced maxima centered at $\vartheta_k \approx 125^\circ$ and 180° . However, the relative intensity of these maxima is now different with the maxima at $\vartheta_k \approx 125^\circ$ becoming noticeably more populated compared to those at $\vartheta_k = 180^\circ$. Besides, the relative importance of the capture into the ground state decreases (as expected).

Figure 4 shows also three more results. The spectrum presented in 4b was obtained by approximating all the states $\chi_{v_a}(\mathbf{r}_1)$, $\chi_{v_a}(\mathbf{r}_2)$ and $\chi_p(\mathbf{r}_2)$ by plane waves, i.e. assuming that both electrons in the initial channel as well as the emitted electron do not feel the HCI's field.

Figure 4c displays results calculated when the states $\chi_{v_a}(\mathbf{r}_2)$ and $\chi_p(\mathbf{r}_2)$ are modelled by plane waves whereas the state $\chi_{v_a}(\mathbf{r}_1)$ is the coulomb one. Thus, in this case we neglect the action of the HCI's field only on that electron, which is not captured.

Finally, figure 4d shows the spectrum obtained if the state $\chi_{v_a}(\mathbf{r}_1)$ is taken as a plane wave but the states $\chi_{v_a}(\mathbf{r}_2)$ and $\chi_p(\mathbf{r}_2)$ are coulomb waves.

When the action of the HCI's field is neglected for both electrons (of course, except in the final bound state χ_b) the calculated spectrum has very pronounced maxima at $\vartheta_k = 180^\circ$ and their intensity rapidly decrease when the transverse component k_{tr} of the electron momentum

increases (see figure 4b).

If the field of the HCI is neglected only for that electron, which is finally emitted, the maxima at $\vartheta_k = 180^\circ$ become less pronounced but new maxima do not yet appear although the calculated spectrum has more extension in the direction of larger k_{tr} (see figure 4c). If we neglect the action of the HCI's field on that electron which is finally captured but take into account HCI's action on the other electron, the calculated spectrum extends even more in the transverse direction but new maxima are still absent (see figure 4d).

And only when the action of the HCI's field on the electrons is fully included, do new maxima appear at $\vartheta_k \approx 125^\circ$ (figure 4a). In this case the maxima at $\vartheta_k = 180^\circ$ further loose in intensity and the (relative) extension of the spectrum in the direction of large k_{tr} is most pronounced.

It follows from these results that the action of the HCI's field on *both* electrons is necessary for the appearance of the second maxima in the emission spectrum. Therefore, the physical origin of these maxima is qualitatively different from that of the EET mechanism, which proceeds via the interaction in the initial channel between the ion and only *one* of the atomic electrons. However, we could not find a simple physical picture for this strong-field mechanism.

The maxima at $\vartheta_k = 180^\circ$ for their appearance need, in principle, neither the interaction with the HCI in the initial channel nor the interaction between the HCI and the emitted electron. According to the results presented in figure 4 the distortion of the initial two-electron state by the field of the HCI and the action of this field on the emitted electron just diminish the EEA mechanism.

Additional information about the transfer-ionization can be obtained by calculating cross sections for this process using the rest frame of the ion. Let us briefly discuss the dependence of the transfer-ionization in this frame on the emission angle. This can be done by studying the cross section $d^2\sigma/d\varepsilon_p \sin\theta_p d\theta_p$, where ε_p and θ_p are the electron emission energy and polar angle in this frame.

In the rest frame of the ion the EEA and EET mechanisms result in the maxima located at $\theta_p \approx 0$ and $\theta_p \approx 45^\circ$, respectively (see figure 5, [22]), where the angle θ_p is counted from the velocity of the atom.

In figures 6-8 the energy-angular distribution is shown for the correlated transfer-ionization in collisions of 22.5 MeV/u Ne^{10+} , Ca^{20+} and Zn^{30+} with helium resulting in electron capture into the ground state of the ion. In all these figures there is one maximum at $\theta_p \approx 0$ corresponding to the EEA, no maximum at $\theta_p \approx 45^\circ$ and the second maximum whose center is located between $\theta_p \approx 20^\circ$ and $\theta_p \approx 30^\circ$. It is seen in the figures that the relative intensity of this maximum (compared to the EEA) strongly increases when the charge of the ion increases.

The center of this maximum slightly moves to lower angles when we go from Ne^{10+} to Ca^{20+} ions but shifts somewhat upwards when Ca^{20+} is replaced by Zn^{30+} . Thus, for a fixed impact velocity of $v = 30$ a.u. the an-

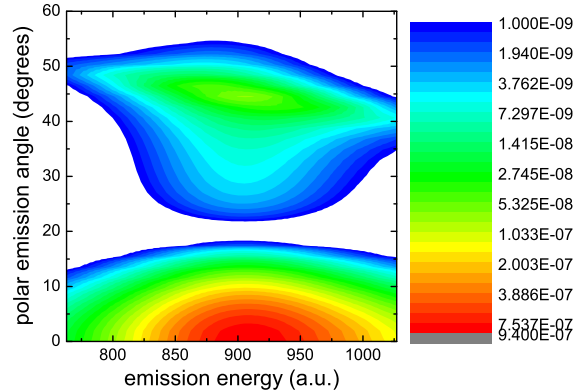


FIG. 5: The energy-angular spectrum $d^2\sigma/d\varepsilon_p \sin\theta_p d\theta_p$ for the reaction $22.5 \text{ MeV } p^+ + \text{He}(1s^2) \rightarrow \text{H}(1s) + \text{He}^{2+} + e^-$. The spectrum is given in the rest frame of the ion.

gular position of this center depends rather weakly (and nonmonotonously) on the charge of the ion when the latter varies in the (quite broad) range $10 \leq Z_i \leq 30$.

In our calculations partial-wave expansions for the states $\chi_{v_a}(\mathbf{r}_1)$, $\chi_{v_a}(\mathbf{r}_2)$ and $\chi_p(\mathbf{r}_2)$ are used [23]. For $Z_i \ll v$ the numbers of the partial waves become very large. Besides, the radial integrands these waves are part of become highly oscillating. All this makes it difficult for us to perform the computation at $Z_i \ll v$ using the Coulomb form for all the states $\chi_{v_a}(\mathbf{r}_1)$, $\chi_{v_a}(\mathbf{r}_2)$ and $\chi_p(\mathbf{r}_2)$. Therefore, at the moment we cannot address an interesting point: whether with decreasing the ratio Z_i/v the second maximum smoothly goes over into the EET or it decreases in intensity and eventually disappears without moving into the region $\theta_p \approx 45^\circ$ where the EET independently arises.

IV. CONCLUSIONS

We have considered transfer-ionization in collisions of helium with fast nuclei having so high charge Z_i that $Z_i \sim v \gg Z_a$. In this consideration we focused on the correlated channels of this process in which the electron-electron interaction during the collision plays a crucial role. Our results were obtained using a treatment which enables one to fully account for the action of the strong field generated by a highly charged ion on electrons, both in the initial and final states of the reaction.

Our consideration shows that the strong field has a very profound effect on the correlated transfer-ionization. Compared to the weak-field regime realized in collisions with fast low charged ions the strong field weakens (in relative terms) the emission of high-energy electrons into the direction (exactly) opposite to the motion of the pro-

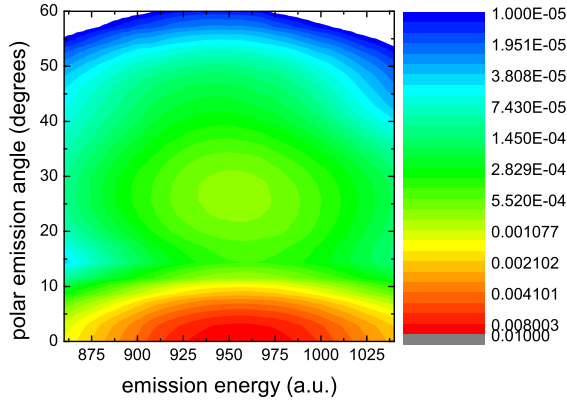


FIG. 6: Same as in figure 5 but for the reaction 22.5 MeV/u $\text{Ne}^{10+} + \text{He}(1s^2) \rightarrow \text{Ne}^{9+}(1s) + \text{He}^{2+} + e^-$.

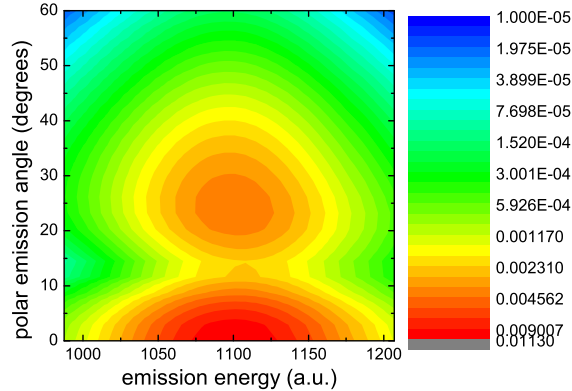


FIG. 7: Same as in figure 5 but for the reaction 22.5 MeV/u $\text{Ca}^{20+} + \text{He}(1s^2) \rightarrow \text{Ca}^{19+}(1s) + \text{He}^{2+} + e^-$.

jectile and strongly suppresses the emission perpendicu-

lar to this motion. Instead, a very substantial part of emission via the correlated channels goes now into the direction around $\vartheta_k \approx 125^\circ$ and its relative importance increases with the strength of the perturbation. This is in contrast to collisions with fast low charged ions where this part of the momentum space is not important at all.

The correlated transfer-ionization is intimately related to the process of radiative two-electron transfer in which two atomic electrons are captured by the projectile with emission of a single photon. Indeed, the electron ejected in the transfer-ionization can undergo radiative recombination with the projectile leading to the radiative two-electron transfer. Since the probability of radiative recombination is very low the latter process has much

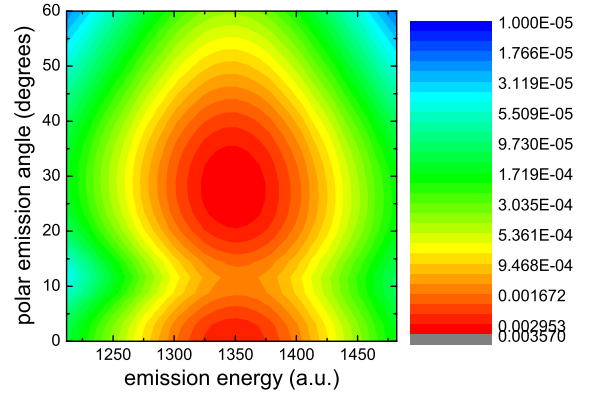


FIG. 8: Same as in figure 5 but for the reaction 22.5 MeV/u $\text{Zn}^{30+} + \text{He}(1s^2) \rightarrow \text{Zn}^{29+}(1s) + \text{He}^{2+} + e^-$.

smaller cross sections than the transfer-ionization that makes it very difficult for experimental observation [24]. Therefore, further theoretical and experimental studies of transfer-ionization [25] may also shed more light on the correlated two-electron-one-photon capture.

The author acknowledges support from the Extreme Matter Institute EMMI.

[1] J.Eichler and W.E.Meyerhof, *Relativistic Atomic Collisions*, Academic Press, New York (1995).
[2] J.H.McGuire, *Electron Correlation Dynamics in Atomic Collisions* (Cambridge University Press, 1997)
[3] N.Stolterfoht, R.D.DuBois, R.D.Rivarola, *Electron Emission in Heavy Ion-Atom Collisions*, Springer, Berlin (1997)
[4] D.S.F. Crothers, *Relativistic Heavy-Particle Collision Theory*, Kluwer Academic/Plenum Publishers, London (2000)
[5] A.B.Voitkiv and J.Ullrich, *Relativistic Collisions of*

Structured Atomic Particles (Springer-Verlag, Berlin, 2008).

[6] A.B.Voitkiv, B.Najjari and J.Ullrich, *Phys.Rev.Lett.* **92** 213202 (2004)
[7] L.H.Thomas, *Proc.R.Soc.* **114** 561 (1927)
[8] A.B.Voitkiv, *J.Phys.* **B 41** 195201 (2008)
[9] V.Mergel et al, *Phys.Rev.Lett.* **86** 2257 (2001)
[10] H.T.Schmidt et al, *Phys.Rev.Lett.* **89** 163201 (2002)
[11] T.Y.Shi and C.D.Lin, *Phys.Rev.Lett.* **89** 163202 (2002)
[12] A.L.Godunov et al, *J.Phys.* **B 37** L201 (2004); **B 38** L123 (2005); *Phys.Rev. A* **71** 052712 (2005)

- [13] H.T.Schmidt et al, Phys.Rev.**A** **72** 012713 (2005)
- [14] A.B.Voitkiv, B.Najjari and J.Ullrich, PRL **101** 223201 (2008)
- [15] M.Schulz et al, PRL **108** 043202 (2012)
- [16] A.B.Voitkiv and X.Ma, Phys. Rev. **A** **86** 012709 (2012)
- [17] L.Gulyas, A. Igarashi and T.Kirchner, Phys. Rev. **A** **86** 024701 (2012)
- [18] M.S.Schöffler et al, arXiv:1208.1324
- [19] J.Briggs and K.Taubjerg, J.Phys. **B** **12** 2565 (1979)
- [20] S.G.Tolmanov and J.H.McGuire, Phys. Rev. **A** **62** 032711 (2000)
- [21] The details of the calculations will be given elsewhere.
- [22] The spectrum shown in figure 3 as well as in 5 was calculated approximating the states $\chi_{\mathbf{v}_a}(\mathbf{r}_2)$ and $\chi_{\mathbf{p}}(\mathbf{r}_2)$ by plane waves.
- [23] unless $\chi_{\mathbf{v}_a}(\mathbf{r}_2)$ and $\chi_{\mathbf{p}}(\mathbf{r}_2)$ are taken as plane waves. In the latter case only the states $\chi_{\mathbf{v}_a}(\mathbf{r}_1)$ and $\chi_b(\mathbf{r}_1)$ are expanded.
- [24] N.Winters, Doctor Thesis, GSI (Darmstadt, Germany, 2013)
- [25] According to the numerous discussions with my colleagues D. Fischer and P. Mokler an experimental verification of our theoretical predictions is feasible.